

# Homogenization of Fiber Composite Material Properties: an Adaptive Multiphysics Implementation

J. Stolz<sup>1</sup>, P. Fideu<sup>2</sup>, A. Herrmann<sup>1</sup>

1. Faserinstitut Bremen e.V., Bremen, Germany

2. Airbus Operations GmbH, Hamburg, Germany

## Introduction

For the manufacturing process of fiber composite parts, various physical phenomena affect the geometry as well as the mechanical and chemical properties of the structure. For development and design of manufacturing processes, thermo-mechanical simulations are used. Here a coupled calculation of heat transfer, mechanical stresses and strains and the curing process of the matrix system are implemented for the determination of process parameters<sup>1,2</sup>. A consideration of the composite part and the process environment, mainly the tooling, is important to get comprehensive and reliable results<sup>3</sup>.

In carbon composite materials the fibers which take the main load of the structural parts are embedded in a shape giving resinous matrix. In this paper, the behavior of an epoxy-based 180°C matrix system, which is typically used for aerospace applications, is investigated. The material has two main phases of matrix and fibers, which can be complemented by further components like e.g. air entrapments, binder materials or thermoplastic veils. Assuming a uniform distribution, the material compound can be treated as porous media. This is crucial to get manageable models when simulating parts with typical sizes. For curing of the resin, the part is heated to a certain temperature and cooled down afterwards to ambient conditions. Through crosslinking of the molecular chains of the epoxy-based matrix, the volume decreases which affects the chemical part of the shrinkage. In addition, with the thermal shrinkage while cooling and through the stiff fibers in the part inner stresses usually occur<sup>4</sup>. This leads to geometry changes after demolding the part from the shape giving tooling. The aim of the calculation is to adapt temperature cycles and tool geometries to achieve high tolerance requirements e.g. in aerospace industry.

For a multiphysics simulation of the composite manufacturing process in an industrial environment, simulation programs have to meet several requirements. Therefore, an intuitive coupling of various physical fields and implementation is essential. Further industrial needs are the handling of

large models and the fast and easy adaption of calculation schemes<sup>5</sup>.

For a macroscopic FEM analysis of the thermomechanical behavior of composite parts, an extensive knowledge about the anisotropic properties of the material compound is essential. Properties of the different components of the porous material have to be homogenized to resulting values for the composite. Here different approaches are available. Also the dependency of material properties to temperature of the part and degree of cure of the matrix system have to be implemented<sup>6,7</sup>.

Various micromechanical analytical models for calculation of effective material properties can be found in literature<sup>8</sup>. The most important are the self-consistent scheme and its evolution, the generalized self-consistent scheme<sup>9,10</sup>, the homogenization analysis method<sup>11-13</sup>, the effective thermoelastic approach<sup>14</sup>, the Mori-Tanaka model<sup>15,16</sup> and the finite-element-method<sup>8,17-20</sup> which is focus of this study.

The approach of homogenization of material properties is based on the use of Representative Volume Elements (RVE). Those unit cells represent a subscale of the heterogeneous material. The single components, which are considered as homogenous, have to be one scale smaller than the RVE. The unit cell is usually chosen as small that averaged material properties show a linear behavior in the RVE.

Assuming the fibers as cylindrical different configuration in a unit cell are possible. In this paper, a body-centered cubic arrangement is chosen. In addition, implementation of more complex RVEs, for example with woven fabrics, is possible.

## Mathematical Model

For thermo-mechanical modeling of composite manufacturing processes, temperature field is used as input field for calculation of thermal strains and stresses. Therefore, a coupling of heat transfer and mechanical modeling is essential.

The heat equation is used for calculation of heat flux and temperature in the domain. Eq. (1) shows the classical heat equation with density  $\rho$ , Temperature  $T$

in  $K$ , specific heat capacity  $C_p$ , thermal conductivity  $k$  and time  $t$ .

$$\frac{k}{\rho * C_p} \Delta T(x, T) = \frac{\partial u}{\partial t} \quad (1)$$

Heat flux  $q$  is calculated by thermal conductivity  $k$  and temperature gradient  $T$  in the according direction (Eq. (2)).

$$q(x, t) = -k(x, t) \frac{dT(x, t)}{dx} \quad (2)$$

For calculation of stress and strains, a linear elastic material model is used. Stresses  $S$  are calculated according to Hooke's law by multiplication of stresses and the stiffness matrix  $C$  (Eq. (4)). Eq. (3) is the equation of motion with stiffness tensor  $F_V$ .

$$0 = \nabla * S + F_V \quad (3)$$

$$S = C * \varepsilon \quad (4)$$

Eq. (5) shows thermal strain tensor  $\varepsilon_{th}$  depending on coefficient of thermal expansion (CTE)  $\alpha$ , temperature  $T$  and reference temperature  $T_{ref}$ .

$$\varepsilon_{th} = \alpha * (T - T_{ref}) \quad (5)$$

Eq. (6) shows homogenization of temperature gradient for calculation of further values. Therefore, the local temperature gradient tensor is integrated over the domain and divided by the volume of the representative volume element.

$$\nabla T_{homogenized} = \frac{\int_{\Omega} \Delta T d\Omega}{\int_{\Omega} d\Omega} \quad (6)$$

Eq. (7) shows homogenization of the heat flux in  $X$ -direction of the spatial coordinate system over the RVE:

$$\dot{Q}_{homogenized} = \frac{\int_{\Omega} Q d\Omega}{\int_{\Omega} d\Omega} \quad (7)$$

Change of Eq. (2) leads to calculation of homogenized thermal conductivity according to Eq. (8).

$$k_{x homogenized} = \frac{\dot{Q}_{homogenized}}{\nabla T_{homogenized}} \quad (8)$$

Homogenization of specific heat capacity is made as shown in Eq. (9) by integration of specific heat capacity over the RVE for calculation of total heat of the domain. Afterwards dividing by volume of the RVW leads to the homogenized specific heat capacity.

$$C_p homogenized = \frac{\int_{\Omega} C_p d\Omega}{\int_{\Omega} d\Omega} \quad (9)$$

Homogenization of coefficient of thermal expansion  $\alpha_{homogenized}$  in longitudinal and transversal to the fibers is made by integration of thermal strain  $\varepsilon_{th}$  in the according room direction (Eq. (10))

$$\alpha_{homogenized} = \frac{\int_{\Omega} \varepsilon_{th} d\Omega}{T - T_{ref}} \quad (10)$$

## Model Implementation

Material properties for carbon fiber and epoxy-based matrix are adapted from literature values<sup>21,22</sup>. As matrix, material RTM6 from Hexcel is used. This epoxy-based matrix system is widely used for aerospace applications. The curing cycle contains heating to 180°C for a time of 90 minutes. As fibers Hexcel G1157, a pseudo-unidirectional carbon fiber reinforcement is used.

Specific heat capacity  $C_{pr}$  of the resin is dependent on temperature  $T$  with a linear influence and degree of cure of the resin depending on glass transition temperature  $T_g$ .  $A_{rcp}$ ,  $B_{rcp}$ ,  $C_{rcp}$ ,  $\Delta_{rcp}$  and  $s$  are fitting parameters. Eq. (11) shows calculation of  $C_{pr}$ <sup>23</sup>. In the present case fully cured resin is assumed with  $T_g$  of 206°C<sup>22</sup>.

$$C_{pr} = A_{rcp} * T + B_{rcp} + \frac{\Delta_{rcp}}{1 + e^{C_{rcp}(T - T_g - s)}} \quad (11)$$

$C_{pf}$  is the specific heat capacity of the resin and calculated with linear influence of temperature  $T$  according to Eq. (6).  $A_{rcp}$ ,  $B_{rcp}$  are fitting parameters<sup>23</sup>.

$$C_{pf} = A_{fcp} * T + B_{fcp} \quad (12)$$

Heat conductivity of the fibers is an anisotropic value differing in fiber direction ( $K_{lf}$ ) and transverse to fiber orientation ( $K_{tf}$ ). Eq. (13), (14) and (15) show calculation of the thermal conductivities<sup>23</sup>.

$$K_{lf} = A_{lf} * T + B_{lf} \quad (13)$$

$$K_{tf} = B_{tf} \quad (14)$$

$$K_r = 0.0008 * T * a^2 - 0.0001 * T * a - 0.0937 * a^2 + 0.22 * a + 0.22 \quad (15)$$

**Table 1:** Material properties and constants of fibre <sup>21,22</sup>

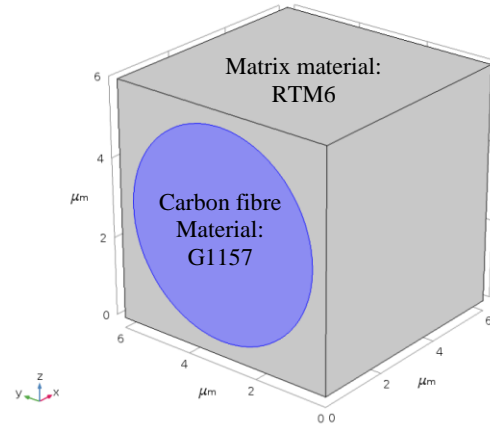
Parameter	Value
Young's modulus longitud.	$E_{f1}=210\,000\text{ N/mm}^2$
Young's modulus transvers.	$E_{f2}=28\,240\text{ N/mm}^2$
Shear modulus	$G_f=50\,600\text{ N/mm}^2$
Poisson's ratio	$\nu_{f12}=0.225$
CTE longitudinal	$\alpha_{f1}=-0.045\cdot 10^{-6}\text{ 1/K}$
CTE transversal	$\alpha_{f2}=12.5\cdot 10^{-6}\text{ 1/K}$
Fitting parameter	$A_{rCp}=0.0023\text{ J/(g}\cdot\text{°C}^2)$
Fitting parameter	$B_{rCp}=0.765\text{ J/(g}\cdot\text{°C}^2)$
Fitting parameter	$A_{rf}=0.0074\text{ W/(m}\cdot\text{°C}^2)$
Fitting parameter	$B_{rf}=9.7\text{ W/(m}\cdot\text{°C}^2)$
Fitting parameter	$B_{rf}=0.84\text{ W/(m}\cdot\text{°C}^2)$

**Table 2:** Material properties and constants of matrix <sup>21,22</sup>

Parameter	Value
Young's modulus	$E_{r1}=2\,890\text{ N/mm}^2$
Shear modulus	$G_r=1\,070\text{ N/mm}^2$
Poisson's ratio	$\nu_{r12}=0.35$
CTE longitudinal	$\alpha_r=65\cdot 10^{-6}\text{ 1/K}$
Fitting parameter	$A_{rCp}=0.0025\text{ J/(g}\cdot\text{°C}^2)$
Fitting parameter	$B_{rCp}=1.80\text{ J/(g}\cdot\text{°C}^2)$
Fitting parameter	$C_{rCp}=1.10\text{ 1/°C}$
Fitting parameter	$\Delta_{rCp}=-0.25\text{ J/(g}\cdot\text{°C}^2)$
Fitting parameter	$S=16.5\text{ °C}$
Glass transition temperature	$T_g=206\text{ °C}$

For mechanical calculation of thermal expansion, the density  $\rho$ , Young's modulus  $E$ , Poisson's ratio  $\nu$  and longitudinal and transversal coefficient  $\alpha_1$  and  $\alpha_2$  are needed. The used values for fiber and matrix system are adapted from literature <sup>21</sup>. Influence of temperature and degree of cure of those parameters are neglected for the present study. Material properties and fitting parameters for Eq. (11)-(15) are reported in Table 1 and Table 2.

For homogenization of material properties, a 3D model is implemented in Comsol Multiphysics. In an RVE a cylindrical fiber is covered by a matrix. Length of the RVE is  $6\mu\text{m}$ , which results in a fiber volume content (FVC) of 60%. Figure 1 shows the model. For most of the calculations, an array of  $6\times 6$  RVEs is used.

**Figure 1:** Single representative volume element with fiber (blue) and matrix (grey)

## Boundary Conditions

For estimation of homogenized material parameters using unit cells, the boundary conditions of the macroscopic system have to be projected on the single unit cell or on a group of them. Depending on the physical influences like applied forces, heat flux, etc. those boundary conditions will have various forms. In this chapter, the boundary condition of a unit cell for calculation of homogenized material properties of specific heat capacity, thermal conductivity and coefficient of thermal expansion are determined.

Homogenization of heat capacity and thermal conductivity is conducted in combination in one model using the Comsol Multiphysics module "heat transfer in solids". Therefore, a time dependent study is used.

A temperature boundary condition at the left side of the model with a 100K higher temperature than the initial temperature of the whole domain heats the RVE. A no flow boundary condition is applied on the remaining edges. Figure 2 shows the boundary condition for determination of values for a heat flow parallel to fibre orientation. Boundary conditions for heat flow transversal to fibre orientation are identical.

$$-nq(B1, B2, B3, B4, B5, B6) = 0 \quad (16)$$

$$T(B4) = 373.15\text{ K} \quad (17)$$

$$T_0 = 273.15\text{ K} \quad (18)$$

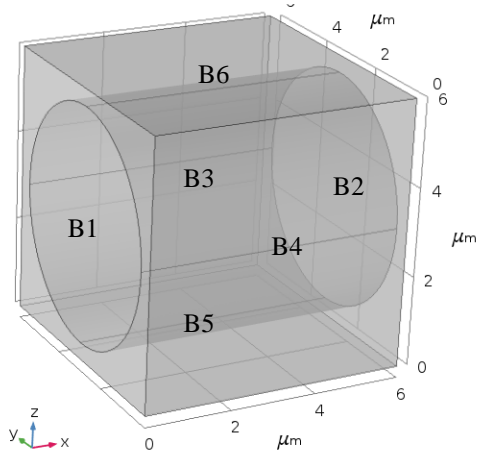


**Figure 2:** Naming of boundaries of RVE

For homogenization of coefficient of thermal expansion, a stationary study and a three-dimensional model are used. Temperature boundary conditions are equal to the ones for determination of heat capacity and thermal conductivity: initial temperature in the domain is 273.15K. Boundary condition of 373.15K at an arbitrary point of the part leads to heating of 100K for the whole domain in the steady study.

The free deformation of the edges of a single RVE does not lead to the result the RVE would have on a compound of cells therefore corresponding boundary conditions are implemented. Therefore, an expansion of the RVE in four direction is allowed, however because of an intended neighbour-RVE the boundaries have to remain straight.

In literature, usually multipoint constraints are used for this kind of boundary conditions. Here the constraints at the node of a boundary are applied to one single external node. In Comsol Multiphysics this can be replaced by use of integration coupling variables. Therefore, the displacements  $u$ ,  $v$ , and  $w$  in the directions  $X$ ,  $Y$  and  $Z$  of a spatial coordinate system are integrated over surfaces of the single boundaries. Eq. (10) - (24) show the boundary equation for boundary boundaries B1-B6.

$$u_0 = \frac{\int_{B1} u dB1}{\int_{B1} dB1} \quad (19)$$

$$u_0 = -\frac{\int_{B2} u dB2}{\int_{B2} dB2} \quad (20)$$

$$v_0 = \frac{\int_{B3} v dB3}{\int_{B3} dB3} \quad (21)$$

$$v_0 = -\frac{\int_{B4} v dB4}{\int_{B4} dB4} \quad (22)$$

$$w_0 = \frac{\int_{B5} w dB5}{\int_{B5} dB5} \quad (23)$$

$$w_0 = -\frac{\int_{B6} w dB6}{\int_{B6} dB6} \quad (24)$$

## Homogenization of Material Properties

### Specific heat capacity and thermal conductivity

Calculation of homogenized heat capacity and thermal conductivity is made for a heating from 0°C to 100°C. Figure 3 shows the temperature field of the model with separated matrix and fibers and a homogenous model with resulting material properties.

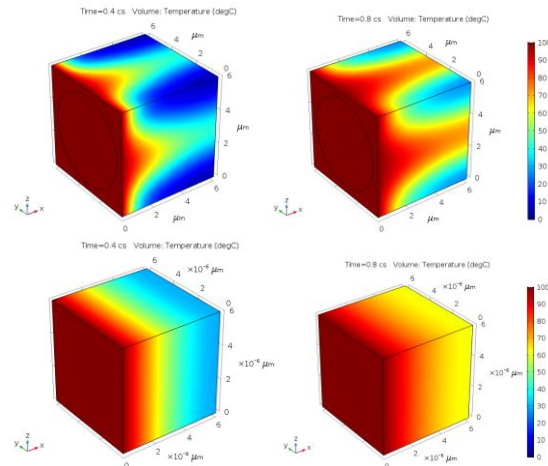


**Figure 3:** Temperature field in the RVE (top) and the homogenized model (bottom) after time of 0.04s (left) and 0.08s (right)

The results are compared with an alternative, numerical calculation method for assuming homogenized values for heat capacity and thermal conductivity using the model of Farmer<sup>24</sup>

In Figure 4 the average temperatures of the RVE, the analytical model and the homogenized cell are compared. Here a good fit of the curves can be seen.

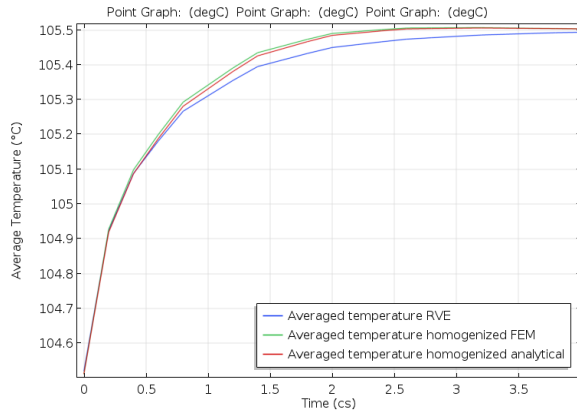


**Figure 4:** Averaged temperatures of RVE and homogenized cell over time

Table 3 Fehler! Verweisquelle konnte nicht gefunden werden. shows the homogenized values longitudinal to fiber orientation calculated with FEM Approach and comparison with analytical result.

**Table 3:** Results of homogenization of material properties for thermal analysis

Value	Analytical	FEM
$k_l$ (W/(m*K))	5.9239	5.2085
$C_p$ (J/(Kg*K))	$1.561 \cdot 10^6$	$1.317 \cdot 10^6$

### Thermal expansion

Figure 5 shows the thermal expansion of a RVE under a temperature change of 100°C with and without constraint of boundary displacement represented by Eq. (19)-(24). The inner cubic represents the original size of the RVE with 800 times of the displacement. This represents a single cell, or rather a cell embedded in a group of RVEs. Table 4 shows the calculation of homogenized values for CTEs calculated using Eq. (10)

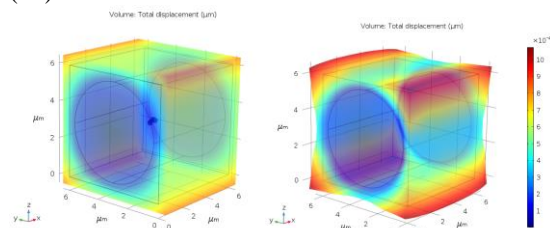


**Figure 5:** Displacement field of RVE at thermal expansion with displacement constraint (top) and without (bottom)

It can be noticed, that in longitudinal direction the fiber has a remarkable influence on the CTE because of the high stiffness. Transversal to fiber CTE is substantially larger because of anisotropic material properties.

**Table 4:** Coefficient of thermal expansion from materials and as result of homogenization

Value	Fiber	Matrix	Homogenized
$\alpha_l$ (1/K)	$-0,45 \cdot 10^{-6}$	$65,0 \cdot 10^{-6}$	$0,624 \cdot 10^{-6}$
$\alpha_t$ (1/K)	$12,50 \cdot 10^{-6}$	$65,0 \cdot 10^{-6}$	$38,0 \cdot 10^{-6}$

In addition to the single unit cell the resulting thermal expansion coefficients of a laminate has been calculated. Therefore a model containing single unit cells in different directions is built up. Figure 6 shows the resulting displacements.

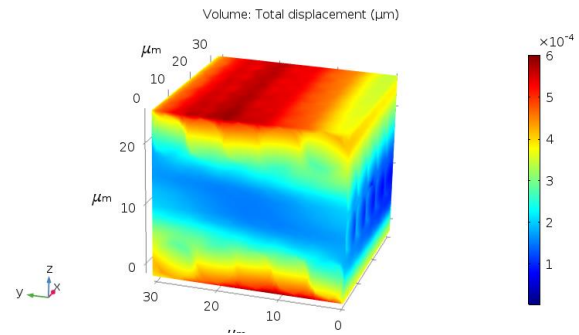


**Figure 6:** Total displacements of a laminate structure

The resulting CTE of  $5.8 \cdot 10^{-6}$  1/K has been compared with calculations basing on the classical laminate theory using the software “eLamX2”. Here a lower value of  $2.9 \cdot 10^{-6}$  1/K. This issue needs further investigation.

### Conclusions

In the present study, the calculation of homogenized material properties for calculation of heat flux and thermal expansions of composite materials using FEM approach is shown. An adaptive model could be set up for calculation of homogenized values of specific heat, thermal conductivity and coefficient of thermal expansion. Especially the boundary condition have to be chosen carefully to get reliable results. For calculation of laminate structure further adaption of the model is needed.

### References

1. Johnston, A. A. An integrated model of the development of process-induced deformation in autoclave processing of composite structures. (University of British Columbia, 1997). doi:10.14288/1.0088805
2. White, S. R. & Hahn, H. T. Process Modeling of Composite Materials: Residual Stress Development during Cure. Part II. Experimental



- Validation. *Journal of Composite Materials* **26**, 2423–2453 (1992).
3. Baran, I., Tutum, C. C., Nielsen, M. W. & Hattel, J. H. Process induced residual stresses and distortions in pultrusion. *Composites Part B: Engineering* **51**, 148–161 (2013).
  4. Brauner, C., Soprano, P., Herrmann, A. S. & Meiners, D. Cure-dependent thermo-chemical modelling and analysis of the manufacturing process of an aircraft composite frame. *Journal of Composite Materials* **49**, 921–938 (2015).
  5. Stolz, J., Fideu, P. & Herrmann, A. ON THE PREDICTIVE ANALYSIS OF FINAL QUALITY OF COMPOSITE PARTS: GAP BETWEEN AVAILABLE MODELS AND INDUSTRIALS NEEDS. in (2018).
  6. Balvers, J., Bersee, H., Beukers, A. & Jansen, K. Determination of Cure Dependent Properties for Curing Simulation of Thick-Walled Composites. in *49th AIAA/ASME/ASCE/AHS/ASC Structures, Structural Dynamics, and Materials Conference, 16th AIAA/ASME/AHS Adaptive Structures Conference, 10th AIAA Non-Deterministic Approaches Conference, 9th AIAA Gossamer Spacecraft Forum, 4th AIAA Multidisciplinary Design Optimization Specialists Conference* (American Institute of Aeronautics and Astronautics, 2006). doi:10.2514/6.2008-2035
  7. McHugh, J., Fideu, P., Herrmann, A. & Stark, W. Determination and review of specific heat capacity measurements during isothermal cure of an epoxy using TM-DSC and standard DSC techniques. *Polymer Testing* **29**, 759–765 (2010).
  8. Dong, K. *et al.* A mesoscale study of thermal expansion behaviors of epoxy resin and carbon fiber/epoxy unidirectional composites based on periodic temperature and displacement boundary conditions. *Polymer Testing* **55**, 44–60 (2016).
  9. Hashin, Z. Analysis of Composite Materials—A Survey. *Journal of Applied Mechanics* **50**, 481 (1983).
  10. Benveniste, Y. Revisiting the generalized self-consistent scheme in composites: Clarification of some aspects and a new formulation. *Journal of the Mechanics and Physics of Solids* **56**, 2984–3002 (2008).
  11. Hiroshi, H. & Minoru, T. Equivalent inclusion method for steady state heat conduction in composites. *International Journal of Engineering Science* **24**, 1159–1172 (1986).
  12. Sakata, S., Ashida, F. & Kojima, T. Stochastic homogenization analysis for thermal expansion coefficients of fiber reinforced composites using the equivalent inclusion method with perturbation-based approach. *Computers & Structures* **88**, 458–466 (2010).
  13. Trung Kien, N., Hai Duyen, N. T. & Chinh, P. D. Equivalent Inclusion Approach and Approximations for Thermal Conductivity of Composites with Fibrous Fillers. in *Proceedings of the International Conference on Advances in Computational Mechanics 2017* (eds. Nguyen-Xuan, H., Phung-Van, P. & Rabczuk, T.) 431–437 (Springer Singapore, 2018).
  14. Hashin, Z. Thermoelastic properties and conductivity of carbon/carbon fiber composites. *Mechanics of Materials* **8**, 293–308 (1990).
  15. Lu, P. Further studies on Mori–Tanaka models for thermal expansion coefficients of composites. *Polymer* **54**, 1691–1699 (2013).
  16. Bohm, H. & Nogales, S. Mori–Tanaka models for the thermal conductivity of composites with interfacial resistance and particle size distributions. *Composites Science and Technology* **68**, 1181–1187 (2008).
  17. Brauner, C., Block, T. B., Purol, H. & Herrmann, A. S. *Microlevel manufacturing process simulation of carbon fiber/epoxy composites to analyze the effect of chemical and thermal induced residual stresses.*
  18. Muliana, A. H. & Kim, J. S. A two-scale homogenization framework for nonlinear effective thermal conductivity of laminated composites. *Acta Mechanica* **212**, 319–347 (2010).
  19. Dong, C. Development of a Model for Predicting the Transverse Coefficients of Thermal Expansion of Unidirectional Carbon Fibre Reinforced Composites. *Appl Compos Mater* **15**, 171–182 (2008).
  20. Xu, Y. & Zhang, W. A strain energy model for the prediction of the effective coefficient of thermal expansion of composite materials. *Computational Materials Science* **53**, 241–250 (2012).
  21. Brauner, C., Block, T. B., Purol, H. & Herrmann, A. S. *Microlevel manufacturing process simulation of carbon fiber/epoxy composites to analyze the effect of chemical and thermal induced residual stresses.* *Journal of Composite Materials* **46**, 2123–2143 (2012).

22. Mesogitis, T. S., Skordos, A. A. & Long, A. C. Stochastic simulation of the influence of cure kinetics uncertainty on composites cure. *Composites Science and Technology* **110**, 145–151 (2015).
23. Skordos, A. A. & Partridge, I. K. Inverse heat transfer for optimization and on-line thermal properties estimation in composites curing. (2004).  
doi:<http://dx.doi.org/10.1080/10682760310001598616>
24. Farmer, J. D. & Covert, E. E. Thermal conductivity of a thermosetting advanced composite during its cure. *Journal of Thermophysics and Heat Transfer* **10**, 467–475 (1996).